

Copolymers of Polyethylene and Perylenediimides through Ring-Opening Metathesis Polymerization

Christian B. Nielsen, Dirk Veldman, Rafael Martín-Rapún, and René A. J. Janssen*

Laboratory of Macromolecular and Organic Chemistry, Eindhoven University of Technology,
PO Box 513, 5600 MB Eindhoven, The Netherlands

Received October 23, 2007; Revised Manuscript Received December 3, 2007

ABSTRACT: The synthesis and characterization of a series of copolymers consisting of polyethylene (PE) and perylenediimide (PERY) dyes is described. The synthetic route comprises metathesis polymerization of *cis*-cyclooctene (COE) and PERY substituted with two allyl groups. This enables incorporating PERY dye molecules into an unsaturated polycyclooctene (PCOE) chain. Subsequent hydrogenation of the PCOE–PERY copolymer affords a high molecular weight PE–PERY copolymer. Ring formation occurs during the metathesis polymerization, but can be suppressed by increasing the initial monomer concentration in accordance with Jacobsen–Stockmayer theory, giving access to predominantly linear PE chains with PERY incorporated in the polymeric chain. Optical characterization of the PE–PERY copolymer with UV–vis absorption and photoinduced absorption spectroscopy reveals that the optical and electronic properties of the PERY moieties are not significantly affected by incorporating them into the polymer chain.

Introduction

Modification of polyethylene (PE) toward materials with distinct thermal characteristics, e.g., glass transition temperature (T_g) and melting temperature (T_m), has attracted significant attention for industrial applications. Likewise, the crystallinity and density are of interest. Lately, this has been illustrated by the introduction of chain shuttling polymerization to prepare linear olefin block copolymers that feature alternating semicrystalline (hard) and amorphous (soft) blocks from a common monomer environment by using a mixture of catalysts.¹ The well-defined ratio of hard (e.g., PE) and soft blocks in these copolymers provides materials that simultaneously have high T_m and low T_g , thus giving materials that have excellent elastomeric properties at high temperatures.¹ Various other characteristics of polyolefins can be tailored by chemical modification, e.g., covalent incorporation of a stabilizer to prevent degradation.² In this respect, color is a property of interest. Polyolefins are often colorless but can be colored by mixing with a dye. An effective approach to avoid migration and phase separation of dye molecules is forming a copolymer by covalently incorporating the dye in the PE chain. This method has the additional advantage of giving control over morphology by varying the relative volumetric ratio of individual covalently bound entities in the copolymer chain.^{3–5} In polymer blends such control of morphology may not be straightforward.





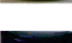

Ring-opening insertion metathesis polymerization (ROIMP) was recently described as a methodology for making AB-alternating copolymers with a high degree of specific alternation.⁶ These polymerizations were carried out by having *cis*-cyclooctene (COE) and a diacrylate present as monomers. Formation of AB-alternating chains was suggested to occur by initial fast ring-opening metathesis polymerization (ROMP)⁷ of COE resulting in polycyclooctene (PCOE), followed by slower cross-metathesis between PCOE and the diacrylate leading to AB-alternating polymers. Efficient cross-metathesis insertion is thus dependent on the reactivity of the diacrylate toward cross-metathesis with PCOE.⁶

In the present work we have focused on copolymers of PE and perylenediimide (PERY) dyes. In its semicrystalline form, PE is mainly present in the orthorhombic phase.⁸ PE was mainly chosen for its abundance in industrial applications, which makes optimization in terms of improved stability and coloring through incorporation of an organic entity interesting. PERYs combine a strong absorption in the visible region with intense fluorescence and high stability against photooxidation and possess interesting electronic properties. For one, PERY films have been shown to display excellent transistor properties⁹ and PE–PERY copolymers could be of interest in the field of “plastic electronics” where the processing properties of the PE part could be envisioned to give working organic transistors similar to block copolymers of PE and poly(3-hexylthiophene) (P3HT).¹⁰ PE–PERY copolymers also may find application in the field of laser welding. Typically PEs are welded by using a dye placed in between two PE surfaces. By having a “colored” PE as dye, an increase in the strength of the weld can be expected due to the structural similarity between the dye (colored PE) and the two PE segments that are welded together. Another reason for choosing PERY as the chromophore is the considerable body of work regarding supramolecular interactions such as π -stacking between PERY moieties or in combination with other chromophores.¹¹ These supramolecular interactions are accompanied by significant changes in the optical absorption and fluorescence spectra. As a consequence, these spectra allow for determining the extent of interactions between the PERY chromophores.

Few polymers have been made where PERYs are incorporated into the main chain. One example is a polytetrahydrofuran–PERY polymer which has been used to study supramolecular interactions in *o*-dichlorobenzene solutions.¹² It was shown that at low temperatures the PERY chromophores are arranged in H-type aggregates. The synthesis of PERY containing polymers is often hampered by low solubility of the resulting polymer, leading to low molecular weights and high polydispersity.¹³ So far, mainly condensation reactions have been used to make PERY containing polymers.^{12–14} It is also the scope of the present work to illustrate a metathesis route to well-defined high molecular weight PE–PERY copolymers.

* Corresponding author. E-mail: r.a.j.janssen@tue.nl.

Table 1. PERY Content, Molecular Weight and Polydispersity of Copolymers PE–PERY(5) (7–11) and PE–PERY(6) (12), Where the Last Column Shows Solutions of the Polymers in Xylenes at ~130 °C

Polymer		C_{PERY}^a (mM)	C_{COE}^a (M)	PERY (wt.%)		M_n^b (kDa)	PDI ^b	PERY/chain		
				Feed	NMR			Feed	NMR	
PE-PERY(5)	7	0.6	1.35	0.4		496	1.32	1.9		
	8	1.3	1.35	0.8		333	1.38	2.9		
	9	3.0	1.35	1.9		185	1.48	3.7		
	10	12.5	1.35	7.4		46	1.60	3.6		
	11	26.2	1.35	14.4	10	18	1.62	2.7	1.9	
PE-PERY(6)	12	6.4	0.62	6.4	2	107	1.93	9.4	2.9	

^a Initial concentration. ^b Measured for the PCOE–PERY precursor.

Experimental Section

General Data. All synthetic procedures were performed under an inert atmosphere of dry argon. Commercial solvents and reagents were used as received unless specified otherwise. THF was degassed with three subsequent freeze–pump–thaw cycles prior to use in polymer synthesis. ¹H NMR and ¹³C NMR were recorded on either a Varian Mercury 400 or Varian Inova 500 spectrometer at 300 K unless specified otherwise. Chemical shifts were referenced to residual solvent signals (¹H: δ = 7.27 ppm and ¹³C: δ = 77.0 ppm for CDCl₃ and ¹H: δ = 6.00 ppm for Cl₂CDCl₂). Data are reported as follows: chemical shift, multiplicity, coupling constants (Hz), and integration. Chromatographic separations using the dry column vacuum chromatography¹⁵ (DCVC) technique were performed on silica gel 60 (SiO₂, particle size 0.015–0.040 mm) using gradient elution (stationary phase/mobile phase). 1,7-Di(4-*tert*-butylphenoxy)perylene-3,4:9,10-tetracarboxydianhydride¹⁶ and 1,7-dibromoperylene-3,4:9,10-tetracarboxydianhydride^{11b} were prepared according to literature procedures. Infrared (IR) spectra were recorded on a Perkin-Elmer Spectrum One FT-IR spectrometer using a Universal ATR sampling accessory. Melting points were determined on a Büchi Melting point B-540 apparatus. Matrix-assisted laser desorption/ionization mass time-of-flight spectra (MALDI–TOF) were obtained using α -cyano-4-hydroxycinnamic acid as the matrix on a PerSeptive Biosystems Voyager-DE PRO spectrometer. DSC measurements were performed on a Perkin-Elmer differential scanning calorimeter Pyris 1 with Pyris 1 DSC autosampler. Melting and crystallization temperatures were determined in the second heating run at a heating/cooling rate of 5 °C·min^{−1}.

Size Exclusion Chromatography. Analytical SEC analyses were performed on a Shimadzu SEC system including a SPD-M10A diode array detector and a RID-10A refractive index detector, using a Polymer Laboratories gel 5 m mixed-D SEC column. THF was used as eluent at a flow rate of 1.0 mL·min^{−1}. The usual sample concentration was ~1 mg·mL^{−1}. Analysis was based on calibration against polystyrene standards.

Film Preparation. Films for photoinduced absorption were made by drop casting a hot (130 °C) solution of the copolymer in xylenes (1 mg·mL^{−1}) onto a quartz plate (cleaned prior to use by UV ozone treatment) held at 130 °C until the solvent had evaporated. Films for UV–vis measurements were prepared in a similar manner but with glass substrates instead of quartz plates.

X-ray. Simultaneous WAXS and SAXS measurements were made using a homemade setup with a rotating anode X-ray generator (Rigaku RU–H300, 18 kW) equipped with two parabolic multilayer mirrors (Bruker, Karlsruhe, Germany), giving a highly

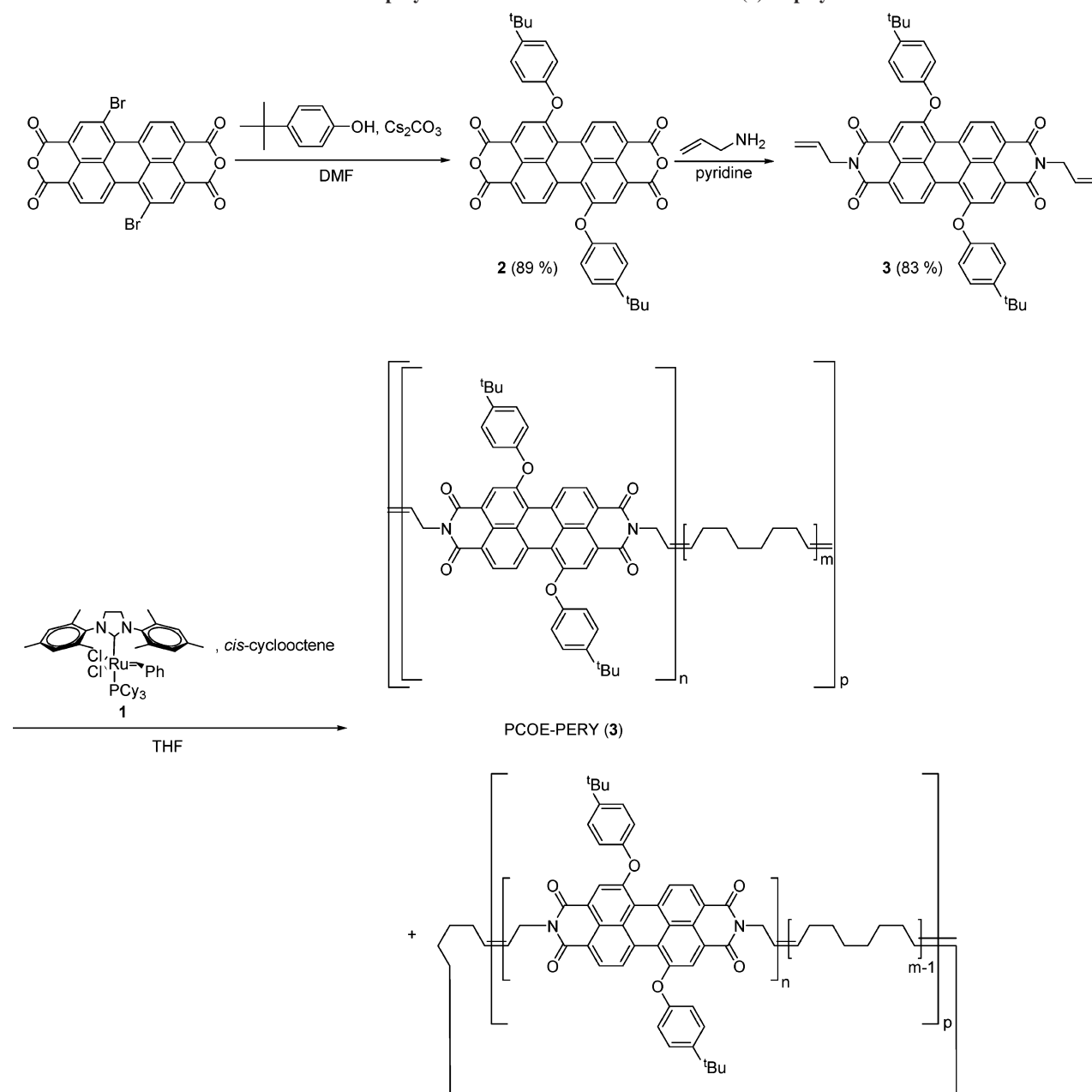
parallel beam (divergence about 0.012°) of monochromatic Cu K α radiation (λ = 0.154 nm). The SAXS intensity was collected with a two-dimensional gas-filled wire detector (Bruker Hi-Star). The WAXS intensity was recorded with a linear position sensitive detector (PSD-50M, M. Braun, Germany). In all cases the crude product was filled in a Lindemann glass capillary (0.9 mm diameter) and mounted in an adapted Linkam THMS 600 hot-stage.

Photoinduced Absorption. Near steady-state photoinduced absorption (PIA) spectra were recorded between 0.30 and 2.3 eV by excitation at 2.35 eV (528 nm) with a mechanically modulated (275 Hz) CW argon ion laser pump beam and measuring the change in transmission of a tungsten–halogen probe beam through the sample (ΔT) with a phase sensitive lock-in amplifier after dispersion by a monochromator and detection using Si, InGaAs, and cooled InSb detectors. The pump power was typically 50 mW with a beam diameter of 2 mm. The PIA signal ($\Delta T \cdot T^{-1}$) was corrected for the photoluminescence, which was recorded in a separate experiment. Samples were held at 80 K in an inert nitrogen atmosphere using an Oxford Optistat continuous flow cryostat.

1,7-Bis(4-*tert*-butylphenoxy)perylene-3,4:9,10-tetracarboxydianhydride (2).¹⁶ A solution of 1,7-dibromoperylene-3,4:9,10-tetracarboxydianhydride^{11b} (1.72 g, 3.1 mmol), 4-*tert*-butylphenol (1.40 g, 9.3 mmol), and Cs₂CO₃ (2.33 g, 7.2 mmol) in DMF (35 mL) was refluxed for 2 h. The reaction mixture was then cooled on an ice-bath and glacial acetic acid was added (25 mL). The precipitated product was collected by filtration and washed with glacial acetic acid and MeOH yielding 1.50 g (70%) of the title compound. ¹H NMR (400 MHz, CDCl₃): δ 9.63 (d, J = 8.7 Hz, 2H), 8.70 (d, J = 8.3 Hz, 2H), 8.28 (s, 2H), 7.53 (d, J = 7.5 Hz, 4H), 7.12 (d, J = 7.1 Hz, 4H), 1.39 (s, 18H). Because of limited solubility, we could not obtain a ¹³C NMR spectrum.

N,N'-Diallyl-1,7-bis(4-*tert*-butylphenoxy)perylene-3,4:9,10-tetracarboxydiimide (3). A solution of 1,7-bis(4-*tert*-butylphenoxy)perylene-3,4:9,10-tetracarboxylic acid dianhydride (2) (1.32 g, 1.92 mmol) in pyridine (150 mL) was heated to 50 °C with stirring. Allylamine (1.06 g, 18.5 mmol) in pyridine (15 mL) was added dropwise and the reaction mixture was refluxed for 3 h. After cooling, celite was added and the solvent was removed *in vacuo*. Purification with DCVC (*n*-heptane/CHCl₃) yielded 1.22 g (83%) of the title compound as a dark red powder: mp 348–350 °C. ¹H NMR (400 MHz, CDCl₃): δ 9.58 (d, J = 8.4 Hz, 2H), 8.56 (d, J = 8.4 Hz, 2H), 8.33 (s, 2H), 7.47 (d, J = 8.8 Hz, 4H), 7.10 (d, J = 8.8 Hz, 4H), 6.03–5.92 (m, 2H), 5.35–5.27 (m, 2H), 5.25–5.18 (m, 2H), 4.81–4.72 (m, 4H), 1.38 (s, 18H). ¹³C NMR (400 MHz, CDCl₃): δ 163.0, 162.7, 155.6, 152.5, 148.3, 133.6, 131.9, 130.2, 129.3, 128.8, 127.5, 124.9, 123.8, 123.7, 123.6, 122.0, 119.2,

Scheme 1. Romp Synthesis of Unsaturated PCOE–PERY(3) Copolymer



117.9, 42.6, 34.6, 31.5; Anal. Calcd for $\text{C}_{50}\text{H}_{42}\text{N}_2\text{O}_6 \cdot (\text{CHCl}_3)_{1/8}$: C, 77.01; H, 5.43; N, 3.58. Found: C, 77.29; H, 5.35; N, 3.78.

***N,N'*-Diallyl-1,7-dibromoperylene-3,4:9,10-tetracarboxydiimide (4).** A solution of 1,7-dibromoperylene-3,4:9,10-tetracarboxydiimide (0.99 g, 1.8 mmol), allylamine (0.32 g, 5.6 mmol), and glacial acetic acid (0.51 g) in *N*-methyl-2-pyrrolidinone (20 mL) was stirred at 85 °C under Ar overnight. After cooling to room temperature, the mixture was poured into MeOH and the precipitated solid was filtered off and washed with glacial acetic acid until the filtrate was light purple to colorless. The filtercake was dissolved in CHCl_3 , celite was added, and the solvent removed *in vacuo*. Purification with DCVC (*n*-heptane/ CHCl_3) yielded 0.45 g (40%) of the title compound as a red powder: no well-defined mp as a mixture of isomers is isolated. ^1H NMR (400 MHz, CDCl_3): δ 9.47 (d, $J = 8.2$ Hz, 0.48H), 9.47 (d, $J = 8.2$ Hz, 2H), 8.92 (s, 0.48H), 8.91 (s, 2H), 8.70 (d, $J = 8.1$ Hz, 0.48H), 8.69 (d, $J = 8.1$ Hz, 2H), 8.92 (s, 0.48H), 6.07–5.94 (m, 2.48H), 5.39–5.33 (m, 2.48H), 5.28–5.23 (m, 2.48H), 4.87–4.80 (m, 4.96H). ^{13}C NMR (400 MHz, CDCl_3): δ 162.9, 162.5, 162.0, 161.7, 138.2, 138.1, 137.5, 136.7, 136.6, 133.3, 133.0, 132.9, 132.5, 131.8, 131.6, 131.4, 130.1, 130.0, 129.2, 128.5, 128.1, 128.0, 126.9, 123.2, 123.0, 122.6,

122.3, 121.7, 120.8, 118.5, 118.2, 118.0, 42.8, 42.7, 42.6; Anal. Calcd for $\text{C}_{20}\text{H}_{16}\text{Br}_2\text{N}_2\text{O}_4 \cdot (\text{CHCl}_3)_{1/3}$: C, 54.53; H, 2.46; N, 4.19. Found: C, 54.32; H, 2.39; N, 4.64.

***N,N'*-Diallyl-1,7-bis[4-(diphenylamino)phenyl]perylene-3,4:9,10-tetracarboxydiimide (5).** A solution of *N,N'*-diallyl-1,7-dibromoperylene-3,4:9,10-tetracarboxydiimide (**4**) (97 mg, 0.15 mmol), 4-(5,5-dimethyl-1,3,2-dioxaborinan-2-yl)-*N,N*-diphenylbenzenamine (120 mg, 0.34 mmol), Na_2CO_3 (0.996 g), and $\text{Pd}(\text{PPh}_3)_4$ (13 mg) was mixed in toluene (20 mL), water (10 mL), and EtOH (5 mL). The reaction was refluxed for 3 days, and water (50 mL) was then added. The quenched reaction mixture was extracted with CH_2Cl_2 (3×50 mL). The combined organic phases were dried (MgSO_4) and celite was added. The solvent was removed *in vacuo*, and DCVC (CH_2Cl_2 /toluene) left 80 mg (54%) of the title compound: mp 332–334 °C. ^1H NMR (400 MHz, CDCl_3): δ 8.65 (s, 2H), 8.27 (d, $J = 8.1$ Hz, 2H), 8.07 (d, $J = 8.1$ Hz, 2H), 7.36 (t, $J = 8.6$ Hz, 4H), 7.33 (d, $J = 7.4$ Hz, 4H), 7.25–7.08 (m, 20H), 6.07–5.95 (m, 2H), 5.37–5.31 (m, 2H), 5.25–5.20 (m, 2H), 4.85–4.79 (m, 4H). ^{13}C NMR (400 MHz, CDCl_3): δ 163.2, 148.5, 147.1, 140.8, 135.4, 135.4, 134.9, 132.5, 132.0, 130.0, 129.7, 129.5, 129.4, 129.192, 127.6, 125.2, 123.8, 123.5, 122.0, 121.6, 117.7, 42.5; A

signal in the ^{13}C NMR spectrum of **5** is missing which is ascribed to accidental isochrony. Anal. Calcd for $\text{C}_{66}\text{H}_{44}\text{N}_4\text{O}_4$: C, 82.83; H, 4.63; N, 5.85. Found: C, 82.37; H, 4.59; N, 5.88.

***N,N'*-Diallyl-1,7-bis(4-*tert*-butylphenyl)perylene-3,4:9,10-tetracarboxydiimide (6).** A solution of *N,N'*-diallyl-1,7-dibromoperylene-3,4:9,10-tetracarboxydiimide (**4**) (98 mg, 0.16 mmol), 2-(4-*tert*-butylphenyl)-5,5-dimethyl-1,3,2-dioxaborinane (0.30 g, 1.2 mmol), Na_2CO_3 (1.054 g), and $\text{Pd}(\text{PPh}_3)_4$ (16.3 mg) was mixed in toluene (20 mL), water (10 mL), and EtOH (5 mL). The reaction was refluxed for 3 days and water (50 mL) was then added. The quenched reaction mixture was extracted with CH_2Cl_2 (3×50 mL) and the combined organic phases were dried (MgSO_4) and celite was added. The solvent was removed *in vacuo*, and DCVC (CH_2Cl_2 /toluene) (two times) left 48 mg (42%) of the title compound: mp $>365^\circ\text{C}$. ^1H NMR (400 MHz, CDCl_3): δ 8.62 (s, 2H), 8.13 (d, $J = 8.1$ Hz, 2H), 7.85 (d, $J = 8.1$ Hz, 2H), 7.50 (d, $J = 8.7$ Hz, 4H), 7.46 (d, $J = 8.5$ Hz, 4H), 6.05 (m, 2H), 5.37–5.30 (m, 2H), 5.25–5.20 (m, 2H), 4.84–4.80 (m, 4H), 1.41 (s, 18H). ^{13}C NMR (400 MHz, CDCl_3): δ 163.3, 163.2, 152.1, 141.1, 139.0, 135.6, 135.2, 132.7, 132.0, 130.1, 129.5, 129.3, 128.7, 127.6, 127.1, 122.0, 121.6, 117.7, 42.5, 34.8, 31.4; Anal. Calcd for $\text{C}_{50}\text{H}_{42}\text{N}_2\text{O}_4 \cdot (\text{CH}_2\text{CH}_2\text{Cl})_{1/3}$: C, 79.24; H, 5.64; N, 3.67. Found: C, 79.22; H, 5.61; N, 3.77.

General Procedure for ROMP. Representative examples and characterizations are given for unsaturated PCOE–PERY(**5**) **11** and PCOE–PERY(**6**) **12**. Perylenediimide (**5**: 21.3 mg, 0.0223 mmol; **6**: 8.72 mg, 0.0117 mmol) and *cis*-cyclooctene (0.15 mL) were dissolved in THF (0.5 mL for COE+**5**, and 1.5 mL for COE+**6**) and blanketed with Ar. Grubbs' second generation catalyst (benzylidene[1,3-bis(2,4,6-trimethylphenyl)-2-imidazolidinylidene]dichloro(tricyclohexylphosphine)ruthenium) was then added (0.2 mL of a $1.0\text{ mg}\cdot\text{mL}^{-1}$ solution) and the reaction mixture was stirred overnight at room temperature. The reaction mixture typically became very viscous shortly after addition of catalyst. Methanol was then added to precipitate the polymer, which was then isolated by filtration and subjected to SEC analysis. After SEC analysis, the polymers were directly subjected to hydrogenation without further characterization.

General Procedure for Hydrogenation. Unsaturated **11** or **12**, *p*-tosylhydrazine (2 g, 11 mmol) and triethylamine (1 g, 10 mmol) were dissolved in xylenes (30 mL). A few crystals of 2,6-di-*tert*-butyl-4-methylphenol were then added and the reaction mixture was stirred overnight at 130°C . After cooling to RT the mixture was quenched with methanol and the precipitated polymer was isolated by filtration and washed with methanol. **11**: ^1H NMR (400 MHz, $\text{ClCD}_2\text{CD}_2\text{Cl}$, 400 K): δ 8.76–8.64 (bs, 2H), 8.39–8.26 (m, 2H), 8.21–8.09 (m, 2H), 7.63–7.08 (m, 28H), 4.41–4.21 (m, 4H), 1.88–0.95 (m). **12**: ^1H NMR (400 MHz, $\text{ClCD}_2\text{CD}_2\text{Cl}$, 400 K): δ 8.73–8.61 (bs, 2H), 8.23–8.13 (m, 2H), 8.05–7.92 (m, 2H), 7.67–7.50 (m, 8H), 4.31–4.18 (m, 4H), 1.93–0.88 (m). Because of low solubility it was not possible to obtain ^{13}C NMR spectra of the polymers. Details of molecular weights are given in Table 1.

Results and Discussion

ROMP has been shown to result in polymers with low polydispersities and gives very good control over the polymer microstructure.⁷ PE polymers made with ROMP (followed by hydrogenation) often originate from polymerizing COE and adding a second (noncyclic) olefin which results in telechelic unsaturated PEs. Without the presence of such a chain transfer agent (CTA) poor polydispersities are obtained.⁷ Grubbs' second generation catalyst, benzylidene[1,3-bis(2,4,6-trimethylphenyl)-2-imidazolidinylidene]dichloro(tricyclohexylphosphine) ruthenium (**1**) is commonly employed in ROMP and will be used in the present work. As we are interested in incorporating PERYs into a PE chain, the obvious approach is then to copolymerize COE with a PERY that has two olefin functionalities, such that PERY acts as CTA in the polymerization, allowing unsaturated PE to further grow off the PERY moiety embedding PERY in

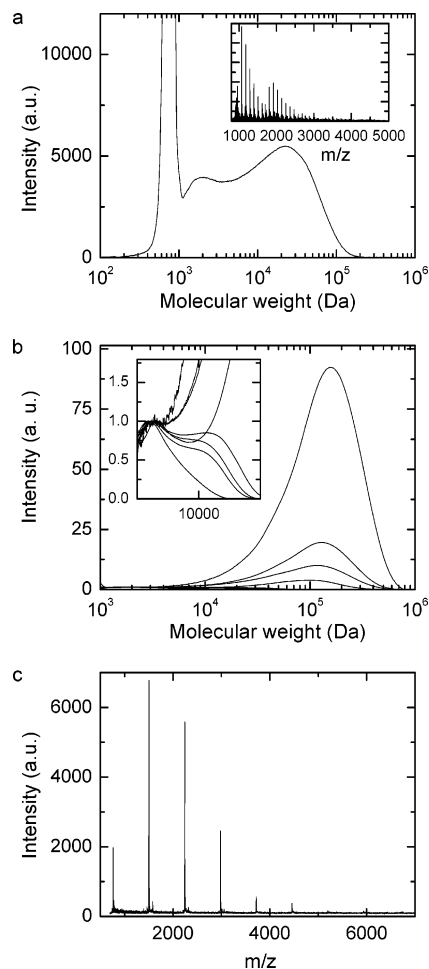


Figure 1. (a) SEC trace (monitored with absorbance measurements at 470 nm) of precipitated PCOE–PERY(**3**) from a polymerization carried out according to Scheme 1. Inset: MALDI–TOF spectrum of the isolated polymer mixture. (b) SEC traces (monitored with absorbance measurements at 470 nm) of the precipitated products from polymerizations carried out according to Scheme 1 at different total concentration and normalized to the low-molecular weight distribution assigned to macrocycles. Inset: magnification around the mass region where mainly macrocycles are observed. (c) MALDI–TOF of the isolated product from a polymerization carried out with only **3**.

the unsaturated PE chain. The fully saturated polymer chain is then obtained by hydrogenation.

Synthesis and Characterization. Initial polymerization experiments were carried out according to Scheme 1. The PERY monomer (**3**) needed for the polymerization was prepared by first reacting 1,7-dibromo-3,4:9,10-perylenetetracarboxylic dianhydride with 4-*tert*-butylphenol to give the phenol substituted PERY derivative (**2**) according to a literature procedure.¹⁶ Subsequently, **2** was reacted with allylamine to form **3** in 83% yield. 1,7-Dibromo-3,4:9,10-perylenetetracarboxydianhydride was prepared by brominating the perylene dianhydride precursor. It is known that this procedure results in approximately 10% of unwanted 1,6-dibromo-3,4:9,10-perylenetetracarboxydianhydride.^{11b} This impurity was carried through in the condensation reaction with 4-*tert*-butylphenol, but it was possible to isolate **3** after column chromatography without any unwanted isomers.

Monomer **3** (0.63 mM) was then subjected to ROMP copolymerization with COE (111 mM) as comonomer using **1** (0.02 mM) as catalyst. After precipitating the reaction mixture in methanol, SEC analysis of isolated PCOE–PERY(**3**) copolymer resulted in the SEC trace shown in Figure 1a. The sharp

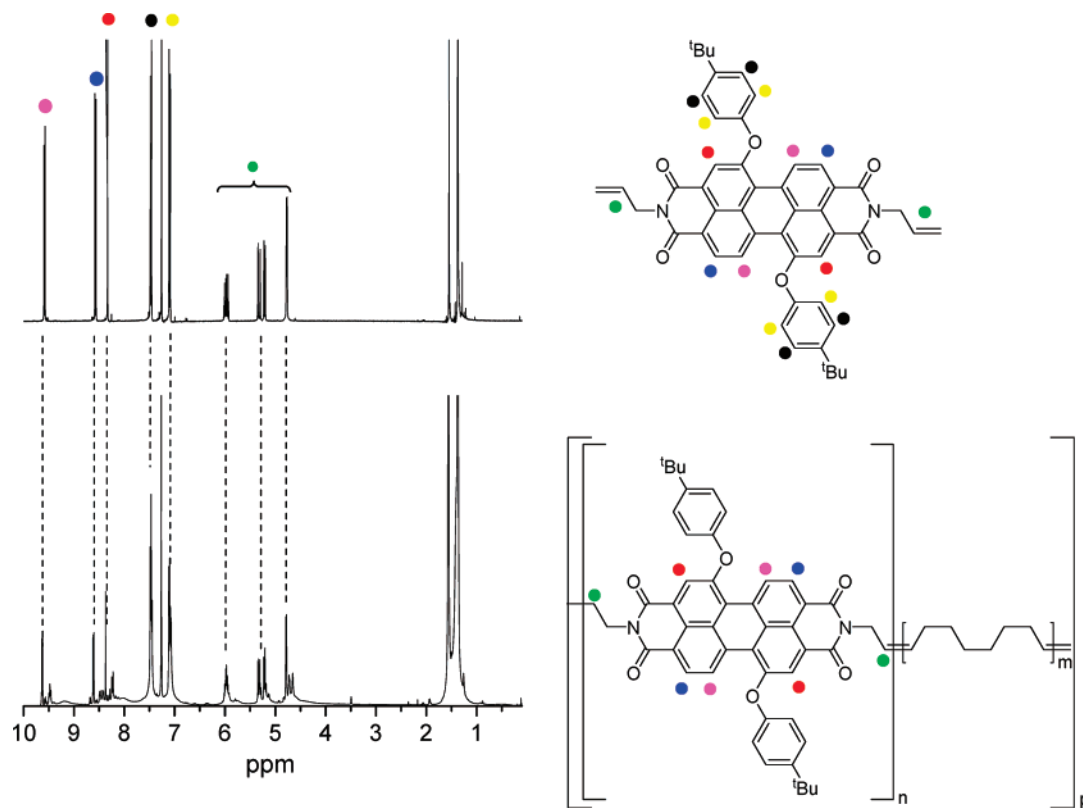
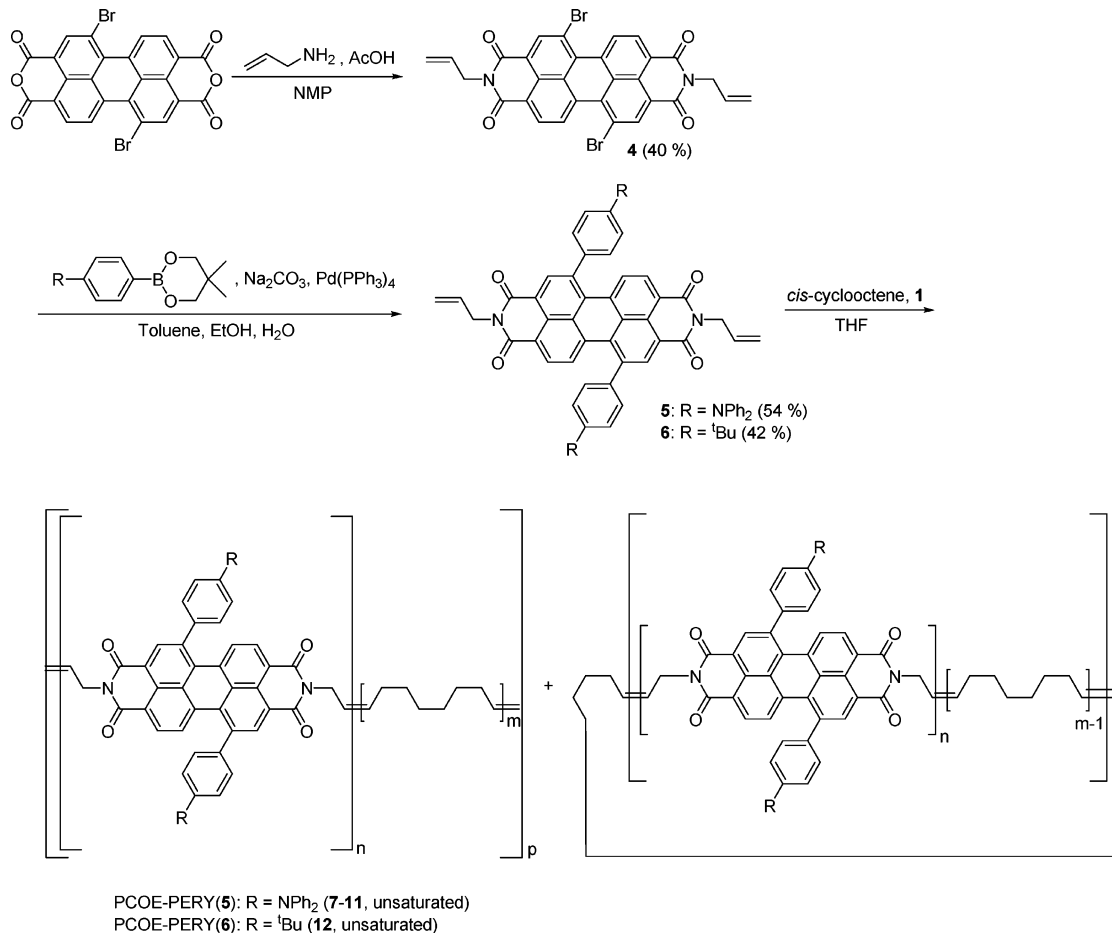


Figure 2. ^1H NMR (25 °C, CDCl_3) of the PERY starting material (3) and PCOE-PERY(3).

Scheme 2. Romp Synthesis of Unsaturated PCOE-PERY(5) and PCOE-PERY(6) Copolymers



intense peak is ascribed to unreacted 3, whereas the two distributions centered at approximately 1200 Da and 20 kDa

are ascribed to macrocycles and linear polymeric chains, respectively. The presence of macrocycles in the isolated product

was confirmed by MALDI–TOF measurements (inset in Figure 1a). The difference in mass between a macrocycle and a linear chain should be 28 Da corresponding to ethylene. The mass distributions observed in the MALDI–TOF spectrum confirm that the low molecular weight distribution can indeed be ascribed to macrocycles ($M_{\text{macrocycles}} = mM_{\text{COE}} + n(M_{\text{PERY}} - M_{\text{C}_2\text{H}_4})$). Because of two methylene end groups, linear chains have higher mass ($M_{\text{linear}} = mM_{\text{COE}} + n(M_{\text{PERY}} - M_{\text{C}_2\text{H}_4}) + M_{\text{C}_2\text{H}_4}$) and these are not observed in the MALDI spectra below 3000 Da. In more detail, two distributions of macrocycles are observed—one with one PERY moiety incorporated into the chain and one distribution with two PERY moieties. In each distribution masses are nicely separated by 110 Da corresponding to an octene moiety and consistent with macrocycles according to the above expression. The smallest macrocycle with either one or two PERY moieties has two COEs in the cycle. In a separate experiment we also attempted to polymerize **3**, which resulted in a distribution of oligomers, illustrated with the MALDI–TOF spectrum in Figure 1c. Even though this did not result in high molecular weight polymer, the experiment illustrates that it is possible to have PERYs positioned next to each other in the polymer chain or macrocycle. Furthermore, the formation of macrocycles also illustrates that PERY does not function merely as “chain-stopper” utilizing only one of the allylic functional groups in the polymerization reaction, but can be incorporated within a PCOE–chain or PCOE–macrocycle. Hence, the copolymerization is, to some extent, a ring-opening insertion metathesis reaction.

^1H NMR experiments were performed on the crude unsaturated PCOE–PERY(**3**) copolymer (Figure 2). The PERY resonances are easily identified in the spectrum of PCOE–PERY(**3**) by comparing with PERY starting material. Resonances arising from allylic and olefin protons are also identified. Because of the presence of olefin protons more resonances occur in PCOE–PERY(**3**) compared to the PERY starting material. Resonances of the aliphatic protons of the *tert*-butyl and methylene groups overlap.

The formation of macrocycles during polymerization reactions is often seen and the equilibrium between linear chains and macrocycles is described by Jacobsen and Stockmayer theory.¹⁷ Accordingly, the relative amount of macrocycles decreases when the initial concentration of monomers increases because it becomes more likely for a polymer chain to react with a monomer than to ring-close and form a macrocycle. To optimize conditions for linear chain polymers, the initial concentrations of PERY(**3**) and COE were varied (~ 0.3 – 7.7 mM and ~ 0.057 – 1.35 M, respectively), keeping their ratio constant (1:177) in all experiments. SEC traces of the isolated polymers from these experiments are shown in Figure 1b, where all traces are normalized to the low-molecular weight distribution assigned to macrocycles (see inset in Figure 1b). Consistent with Jacobsen–Stockmayer theory¹⁷ we observe a relative decrease in the amount of macrocycles compared to linear chain polymers when the initial concentration of monomers is increased. Also, a higher molecular weight of linear chain polymers is observed upon decreasing the amount of formed macrocycles.

The phenol substituent on the PERY(**3**) core is not well-suited for the synthesis of saturated PE–PERY copolymers because phenol groups cannot withstand hydrogenation of the double bonds of intermediate unsaturated PCOE–PERY formed in the ROMP reaction. For this reason we synthesized PERY analogs **5** and **6** where the phenyl substituent is attached to the PERY core by a C–C bond (Scheme 2). 1,7-Dibromo-3,4,9,10-perylenetetracarboxydianhydride was reacted with allylamine

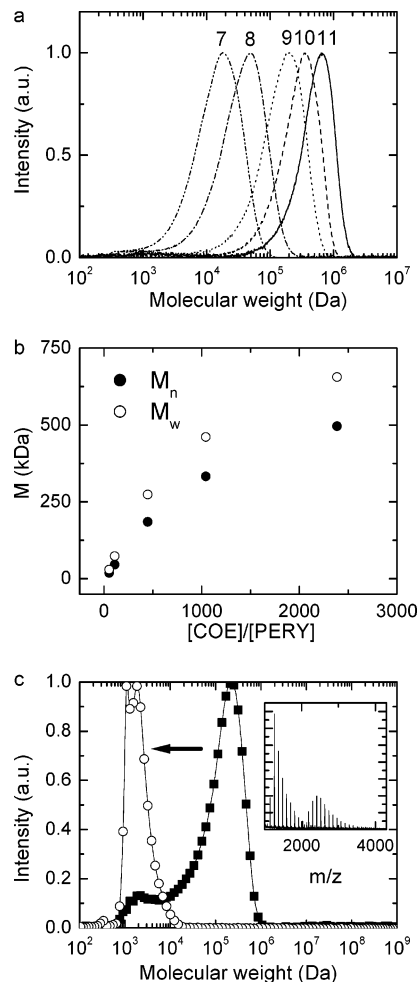
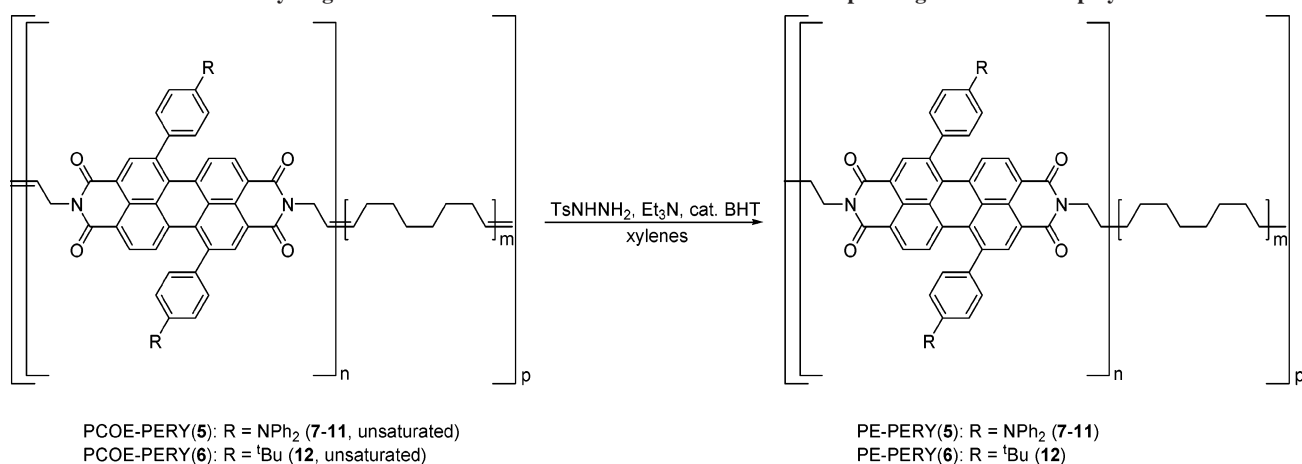


Figure 3. (a) SEC traces (in THF, UV–vis detection, calibrated with polystyrene standards) of the unsaturated PCOE–PERY(**5**) polymers (**7**–**11**) showing one distribution for each polymer. (b) M_n and M_w values of the PCOE–PERY(**5**) polymers. (c) “Redissolving” experiment, where a polymerization was carried out in concentrations that mainly give linear chains, with minor formation of macrocycles. The reaction mixture was then diluted 10 times, and a fresh amount of catalyst was added, resulting in a SEC trace that showed a peak centered at lower molecular weight. The inset shows the MALDI–TOF spectrum of polymers obtained under dilute conditions, confirming that macrocycles are formed.

to give **4** in 40% and Suzuki cross-coupling reactions afforded either PERY derivatives **5** in 54% or **6** in 42% yield. PERY derivatives substituted with 4-(diphenylamino)phenyl substituents as in **5** have previously been investigated and these have been shown to have distinct charge-transfer (CT) bands in their UV–vis spectra.¹⁸ For these PERY derivatives such bands are particularly sensitive to aggregation¹⁹ and, hence, changes in aggregation can be observed when comparing solution and solid state (e.g., films) by monitoring spectral shifts of the CT band.

Using a relatively high initial concentration of COE (1.35 M), we performed a series of polymerizations with **5** and COE (Table 1). At these high concentrations, we observed an increase in viscosity of the mixture during the reaction to an extent where it was difficult to obtain efficient stirring. SEC traces of isolated unsaturated PCOE–PERY(**5**) copolymers are shown in Figure 3a, where we observe an insignificant amount of lower molecular weight macrocycles and a dominant distribution of linear polymer chains. M_n values range from 18 kDa to 500 kDa and polydispersities are in the range from ~ 1.3 to 1.6.

Scheme 3. Hydrogenation of Unsaturated PCOE–PERY to the Corresponding PE–PERY Copolymers



The molecular weight of telechelic polymers made via ROMP is usually controlled by varying the ratio of monomer and CTA,⁷ and often a linear relation is observed between M_n and this ratio.²⁰ For PCOE–PERY(5) this linear correlation is not observed (Figure 3b), and we tentatively ascribe this to incorporation of more perylene units in one chain. The PERYs in this study are bifunctional, such that they can be incorporated into the unsaturated PCOE chain multiple times, which is supported by the observation of macrocycles with two units in MALDI–TOF (inset in Figure 1a).

The formation of macrocycles and the applicability of Jacobson–Stockmayer theory¹⁷ to the synthesis of unsaturated

PCOE–PERY copolymers was investigated by carrying out a simple dilution experiment. A polymerization was carried out with concentrations of 4.9 mM and 1.35 M of **5** and COE, respectively and a concentration of 0.3 mM of **1**. These initial concentrations were chosen such that linear polymer chains form predominately as evidenced from SEC (Figure 3c). This reaction mixture was then diluted to 10 times its volume and the same amount of catalyst was added. After the reaction was completed, the SEC trace exclusively showed distributions of macrocycles which was further confirmed by MALDI–TOF (inset in Figure 3c). These findings lend support to the Jacobsen–Stockmayer theory¹⁷ and to the interpretations

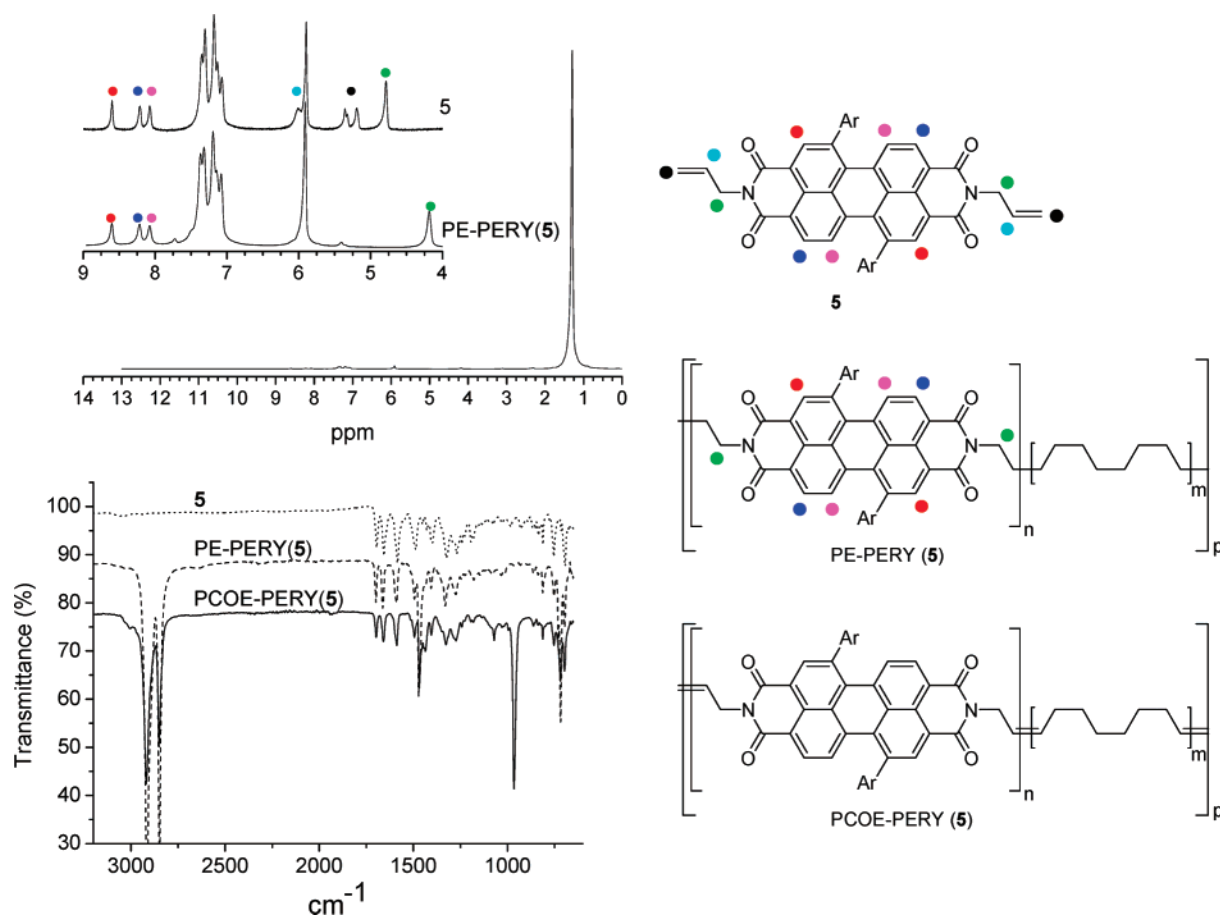


Figure 4. ¹H NMR spectrum (140 °C, TCE-*d*₂) of saturated PE–PERY(5) (Ar = –PhNPh₂) polymer (top left). The inset shows a magnification of the aromatic region of the polymer (bottom inset) and a spectrum of perylene monomer (top inset). IR spectra of saturated PE–PERY(5) (Ar = –PhNPh₂) and unsaturated PCOE–PERY(5) polymer (bottom left).

of the polymerization experiments carried out in the present work.

As we can successfully synthesize linear chains of unsaturated PCOE–PERY copolymers we were interested in saturating the PCOE segments by hydrogenation to obtain saturated PE–PERY. This can conveniently be done by reacting unsaturated polymer with *p*-tosylhydrazine and triethylamine (Scheme 3), which affords the saturated polymer in quantitative yields.

By fully saturating the PE chains we obtain polymers that are considerably less soluble than the unsaturated ones. The efficiency of the hydrogenations was monitored with FT-IR, and exhaustive hydrogenation was confirmed by disappearance of the characteristic alkene C–H bend vibration at 966 cm^{-1} , which is present in the unsaturated polymer (see Figure 4).

The actual content of PERY in the final saturated PE–PERY chains can be found from ^1H NMR experiments because the protons of the PE segments only show a single resonance in the aliphatic region (1.30 ppm), whereas the PERY moieties only have resonances in the aromatic region. Because of low solubility of the copolymers, NMR experiments had to be performed in tetrachloroethane- d_2 at $140\text{ }^\circ\text{C}$. For comparison we also recorded an NMR spectrum of **5** under the same conditions. The spectra are shown in Figure 4.

By comparing the integrated NMR signals in the aromatic region to PE resonances, the weight percentage of PERY in PE–PERY(**5**) copolymer (**11**) was determined to be ca. 10%, i.e. somewhat less than the weight percentage (14.4%) in the reaction feed. We assume that for the other PE–PERY(**5**) polymers similar deviations occur between weight percentage in the feed (Table 1) and the actual values. For PE–PERY(**6**) copolymer (**12**), there is a more substantial difference between the weight percentage of the feed (6.4%) and the experimental value determined by NMR (2%). One explanation is that these differences originate from an incomplete incorporation of the PERY monomer in the copolymers even though no or insignificant residual traces of PERY were seen in the SEC traces. The polymers are purified by precipitation in the final step and as shown above lower molecular weight homologues contain 1–3 PERYs in the macrocycle or polymer chain. Upon precipitation of higher molecular weight polymer chains while leaving lower molecular weight homologues in solution, the amount of PERY in the precipitate decreases relative to the feed ratio. This line of reasoning is supported by the observation of a slightly colored solution after collecting the precipitate. Another reason for the differences observed between feed ratio and composition inferred from NMR, is the accuracy of the NMR experiment as integrated signals are not accurate to more than 5%. For this particular reason we are cautious to report NMR results for the PERY contents for the remaining polymers. The experiments suggest, however, a slightly lower PERY content in the copolymer than calculated from the feed ratio.

From the weight percentages of PERY (from either reaction feed or NMR) and number-averaged molecular weights of the polymers a rough estimate of the average number of PERY moieties per chain can be obtained (Table 1). These numbers show that even when assuming efficient incorporation of PERY moieties into the polymer chain, the actual number of PERYs per chain is only 2–4, with actual values based on being slightly less (2–3).

In addition to the results from FT-IR, the NMR spectrum of hydrogenated PE–PERY(**5**) polymer also confirms exhaustive hydrogenation as resonances from allylic protons (6.01 ppm) are not observed (see Figure 4, the signal at 5.91 ppm is due to TCE- d_2).

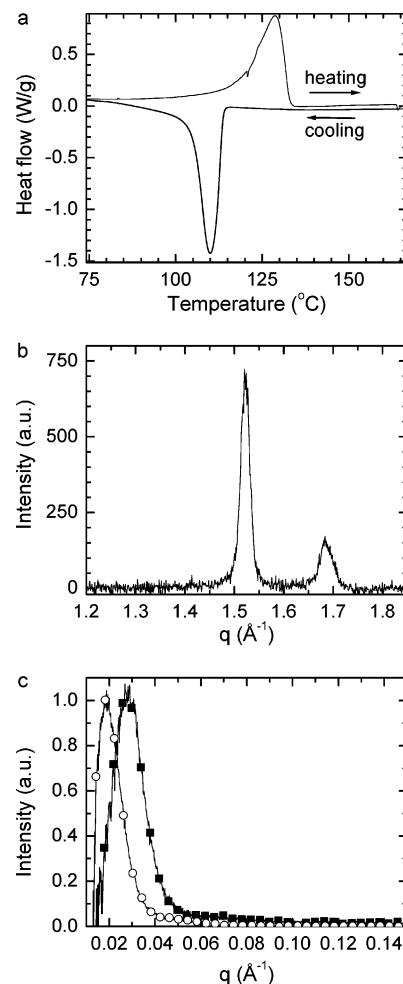


Figure 5. (a) DSC trace ($5\text{ }^\circ\text{C/min}$) of **7**. The typical melting endotherm and cooling exotherm for high-density PE are seen. (b) WAXS of **9**. (c) SAXS of **9** (circles) and **11** (filled squares).

DSC measurements were performed to investigate whether PE–PERY polymers retained the thermal and semicrystalline properties that pure PE possesses. The DSC trace of **7** (PE–PERY(**5**)) (second heating and cooling runs) shown in Figure 5a was found to be similar to that of high-density PE with a peak melting temperature of $129\text{ }^\circ\text{C}$ and crystallization temperature of $110\text{ }^\circ\text{C}$. Similar DSC traces were obtained for all PE–PERY copolymers.

Powder XRD measurements were also carried out to confirm that PE in the PE–PERY copolymers is semicrystalline. The WAXS profiles of all the polymers exhibit the 110 and 200 reflections of semicrystalline PE as shown for **9** in Figure 5b.^{8c} SAXS measurements were only performed on **9** and **11** (Figure 5) and display a broad maximum, whose position is apparently dependent on the content of PERY in the polymer, which is then inherently dependent on M_n of the polymer. The maxima correspond to real space distances of $\sim 33\text{ nm}$ for **9** and $\sim 23\text{ nm}$ for **11**. These distances could originate from large scale ordering, possibly reflecting sizes of the crystalline domains in the polymer samples.^{8c} Another interpretation is that they correspond to the average distance between hard PERY stacks.

So far we have illustrated by DSC and X-ray measurements that the PE–PERY polymers behave similar to PE. In a visual illustration of this, we prepared a film of **12** by heating the neat polymer above the melting temperature of PE ($129\text{ }^\circ\text{C}$) and melt pressed the polymer between two glass plates which resulted in the film shown in Figure 6. This simple experiment illustrates

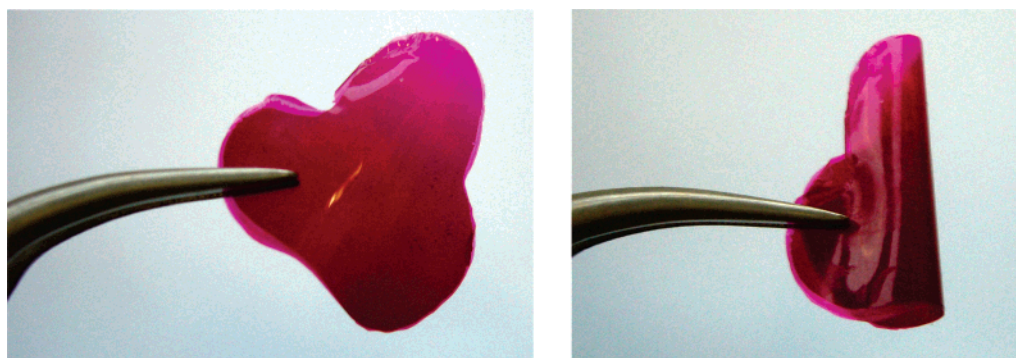


Figure 6. Film made of **12** by heating a sample in between two glass plates to $\sim 140^\circ\text{C}$ and applying pressure.

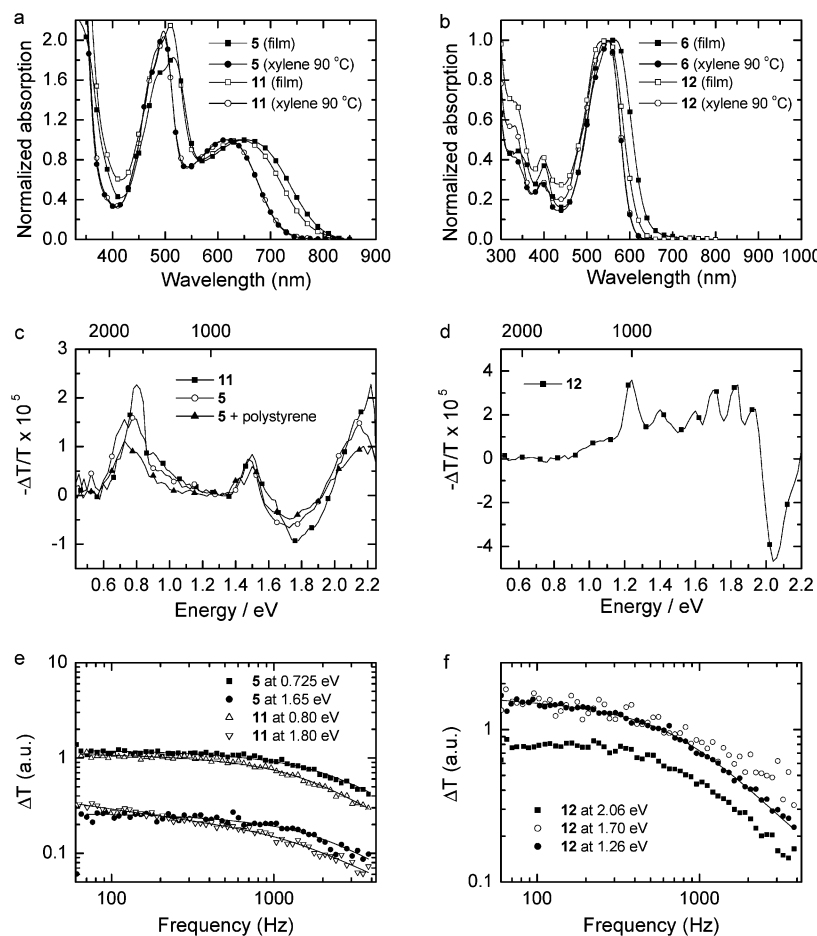


Figure 7. (a) UV-vis spectra of **5** and **11** in both solution (xylenes at 90°C) and as film. (b) UV-vis spectra of **6** and **12** in both solution (xylenes at 90°C) and as film. (c) PIA spectra of **11** and **5** as films recorded at 80 K. A PIA spectra of **5** embedded in polystyrene recorded at 80 K is also included for comparison. (d) PIA spectrum of a film of **12** recorded at 80 K. The resolved peaks in the 1.6–1.9 eV region are in part due to imperfect correction of the photoluminescence, which is 10 times higher than the PIA in this range. (e) Modulation frequency dependence of the change in transmission at 0.725 and 1.65 eV for **5** and at 0.80 and 1.80 eV for **11**. (f) Modulation frequency dependence of the change in transmission at 1.26 eV, 1.70 eV and at 2.06 eV for **12**. The solid lines are fits to the data used to determine the lifetimes.

the ease by which the polymeric material can be processed. By applying more advanced processing (e.g., using a commercial compression molder) film thicknesses in the range of 100 nm can be obtained.²¹

Electronic Interactions in the Solid State. The UV-vis absorption spectra of PE-PERY polymers (**11** and **12**) and of the corresponding monomers (**5** and **6**) recorded in xylenes solution at 90°C and as thin films are depicted in Figure 7,

The solution phase absorption spectra of **5** and **11** exhibit a charge-transfer absorption (CT) band at $\sim 620\text{ nm}$ (Figure 7, parts a and b), which most likely originates from the interaction between the electron-rich triphenylamine and the electron-deficient PERY core aromatic system. This CT band broadens

and shifts to lower energies in the spectra of films of both **5** and **11** suggesting aggregation of PERY moieties in both films. The smaller shift for **11** compared to **5**, suggests that aggregation of PERY(**5**) moieties is less in the copolymer than in the monomer film. From the apparent onsets in the CT bands we can deduce energies of ~ 1.7 and $\sim 1.55\text{ eV}$ for the nonaggregated and aggregated CT state of PERY, respectively. The differences between solid state and solution-phase spectra are smaller for the absorption spectra of **6** and **12**. For monomer **6**, there is a small but distinct red shift in the solid state, but for PE-PERY(**6**) copolymer **12**, the bands at 550 nm are virtually identical in solution and film, indicating that aggregation is less pronounced.

Photoinduced absorption spectroscopy (PIA) confirms the CT character of the lowest excited-state of polymer **11** (Figure 7c). Upon photoexcitation two induced absorptions appear at 0.75 eV and at 1.50 eV that are characteristic of triphenylamine radical cations and PERY radical anions respectively, together with a photobleaching band at 1.75 eV. At 80 K, the lifetime of the charge separated state in **11** is about 250 μ s as determined by analysis of the modulation frequency dependence of the PIA signal (Figure 7e). A similar PIA spectrum and lifetime (\sim 170 μ s) was obtained for monomer **5** (Figure 7, parts c and e). In further characterizing the dependence of the electronic properties of the triphenylamino-substituted perylene moiety on the molecular environment, we recorded a PIA spectrum of **5** embedded in a polystyrene matrix (Figure 7c). By comparing the PIA spectra of **5** and **11**, we only observe subtle changes in optical properties; small intensity differences are seen in between the PIA spectra, but these are too small to be of importance in conclusive arguments.

The PIA spectrum of the 4-*tert*-butylphenyl substituted polymer **12** (Figure 7d) is distinctively different from the spectrum of **11** and exhibits a series of resolved transitions. The lifetime of each of the absorption bands is similar and amounts to \sim 300–400 μ s (Figure 7f). On the basis of comparison with literature,²³ we assign the lowest energy transitions (1.06, 1.24, and 1.40 eV) to radical anions and the transitions at higher energy (1.6–1.9 eV) to radical cations of the PERY moieties in polymer **12**.

Conclusions

A series of PE–PERY copolymers has been synthesized via ROMP of COE and diallyl–PERY dyes followed by hydrogenation under mild conditions. Ring formation was shown to occur during the metathesis polymerization, but could be suppressed by increasing the initial monomer concentration in accordance with Jacobsen–Stockmayer theory, giving access to predominantly linear polyethylene chains with PERY moieties incorporated in the polymeric PE chain. The observed decrease of molecular weight with increasing relative concentration of diallyl–PERY monomer, suggests that this primarily acts as a CTA in a secondary metathesis reaction after the fast ROMP of PCOE. The limited number of PERY units per PE–PERY chain in the final product indicates that the insertion (ROIMP) mechanism of diallyl–PERY into PCOE may occur, but is not predominant. Optical properties of the polymers reveal that the interactions between chromophores in the solid state are only slightly influenced by incorporating the PERY moiety in a PE chain.

The PE–PERY copolymers combine the processing advantages of polyethylene and the optical properties of perylenediimides. Further studies will be directed to explore the use of these new copolymers as functional materials for opto-electronic applications.

Acknowledgment. We thank Dr. O. A. Sherman and Dr. C. P. Radano for fruitful discussions. This work, as part of the European Science Foundation EUROCORES Programme SONS was supported by funds from NWO and the EC Sixth Frame-

work Programme. D.V. acknowledges support from the NAIMO EU integrated project (NMP4-CT-2004-500355). R.M.-R. is funded by an EU Marie Curie Intra-European Fellowship (Project MEIF-CT-2006-042044) within the EC Sixth Framework Programme.

References and Notes

- Arriola, D. J.; Carnahan, E. M.; Hustad, P. D.; Kuhlman, R. L.; Wenzel, T. T. *Science* **2006**, *312*, 714.
- Wilén, C.-E.; Luttkhedde, H.; Hjertberg, T.; Näsman, J. H. *Macromolecules* **1996**, *29*, 8569.
- Bates, F. S.; Fredrickson, G. H. *Annu. Rev. Chem.* **1990**, *41*, 525.
- Bates, F. S.; Schulz, M. F.; Khandpur, A. K.; Förster, S.; Rosedale, J. H.; Almdal, K.; Mortensen, K. *Faraday Discuss.*, **1994**, *98*, 7.
- Matsen, M. W.; Bates, F. S. *Macromolecules* **1996**, *29*, 1091.
- Choi, T.-L.; Rutenberg, I. M.; Grubbs, R. H. *Angew. Chem., Int. Ed.* **2002**, *41*, 3839.
- For recent reviews on ROMP, see: (a) Ivin, K. J.; Mol, J. C. *Olefin Metathesis and Metathesis Polymerization*; Academic Press, San Diego, CA, 1997. (b) Grubbs, R. H.; Khosravi, E. *Mater. Sci. Technol.* **1999**, *20*, 65. (c) Buchmeiser, M. R. *Chem. Rev.* **2000**, *100*, 1565.
- (a) Tashiro, K.; Sasaki, S.; Kobayashi, M. *Macromolecules* **1996**, *29*, 7460. (b) Russel, K. E.; Hunter, B. K. *Polymer* **1997**, *38*, 1409. (c) Gedde, U.; Mattozzi, A. *Adv. Polym. Sci.* **2004**, *169*, 29.
- An, Z.; Yu, J.; Jones, S. C.; Barlow, S.; Yoo, S.; Yoo, S.; Domercq, B.; Prins, P.; Siebbeles, L. D. A.; Kippelen, B.; Marder, S. R. *Adv. Mater.* **2005**, *17*, 2580.
- (a) Müller, C.; Goffri, S.; Andreasen, J. W.; Breiby, D.; Chanzy, H. D.; Janssen, R. A. J.; Nielsen, M. M.; Radano, C. P.; Siringhaus, H.; Smith, P.; Stingelin-Stutzmann, N. *Adv. Funct. Mater.* **2007**, *15*, 2674. (b) Radano, C. P.; Scherman, O. A.; Stingelin-Stutzmann, N.; Müller, C.; Breiby, D. W.; Smith, P.; Janssen, R. A. J.; Meijer, E. W. *J. Am. Chem. Soc.* **2005**, *127*, 12502.
- (a) For a review about supramolecular interactions of perylenediimides, among other systems, see: Hoeben, F. J. M.; Jonkheijm, P.; Meijer, E. W.; Schenning, A. P. H. J. *Chem. Rev.* **2005**, *105*, 1491. (b) Ahrens, M. J.; Sinks, L. E.; Rybtchinski, B.; Liu, W.; Jones, B. A.; Giaimo, J. M.; Gusev, A. V.; Goshe, A. J.; Tiede, D. M.; Wasielewski, M. R. *J. Am. Chem. Soc.* **2004**, *126*, 8284.
- (a) Neuteboom, E. E.; Janssen, R. A. J.; Meijer, E. W. *Synth. Met.* **2001**, *121*, 1283. (b) Neuteboom, E. E.; Meskers, S. C. J.; Meijer, E. W.; Janssen, R. A. J. *Macromol. Chem. Phys.* **2004**, *205*, 217.
- Quante, H.; Schlichting, P.; Rohr, U.; Geerts, Y.; Müllen, K. *Macromol. Chem. Phys.* **1996**, *197*, 4029.
- Karayannidis, G.; Stamelos, D.; Bikiaris, D. *Macromol. Chem.* **1993**, *194*, 2789.
- Pedersen, D. S.; Rosenbohm, C. *Synthesis* **2001**, *16*, 2431.
- Ishi-i, T.; Murakami, K.-i.; Imai, Y.; Mataka, S. *Org. Lett.* **2005**, *7*, 3175.
- (a) Jacobsen, H.; Stockmayer, W. H. *J. Chem. Phys.* **1950**, *18*, 1600. (b) Jacobsen, H.; Beckmann, C. O.; Stockmayer, W. H. *J. Chem. Phys.* **1950**, *18*, 1607.
- Chao, C.-C.; Leung, M.-k.; Su, Y. O.; Chiu, K.-Y.; Lin, T.-H.; Shieh, S.-J.; Lin, S.-C. *J. Org. Chem.* **2005**, *70*, 4323.
- Rybtchinski, B.; Sinks, L. E.; Wasielewski, M. R. *J. Am. Chem. Soc.* **2004**, *108*, 7497.
- (a) Scherman, O. A.; Kim, H. M.; Grubbs, R. H. *Macromolecules* **2002**, *35*, 5366. (b) Hillmyer, M. A.; Grubbs, R. H. *Macromolecules* **1995**, *28*, 8662. (c) Hillmyer, M. A.; Grubbs, R. H. *Macromolecules* **1993**, *26*, 872. (d) Lynn, D. M.; Mohr, B.; Grubbs, R. H. *J. Am. Chem. Soc.* **1998**, *120*, 1627.
- Fornes, T. D.; Hunter, D. L.; Paul, D. R. *Macromolecules* **2004**, *37*, 1793.
- (a) Li, A. D. Q.; Wang, W.; Wang, L.-Q. *Chem.—Eur. J.* **2003**, *9*, 4594. (b) Kasha, M.; Rawles, H. R.; El-Bayoumi, M. A. *Pure Appl. Chem.* **1965**, *11*, 371. (c) Langhals, H.; Jona, W. *Angew. Chem., Int. Ed.* **1998**, *37*, 952. (d) Langhals, H.; Ismael, R. *Eur. J. Org. Chem.* **1998**, 1915.
- Ford, W. E.; Hiratsuka, H.; Kamat, P. V. *J. Phys. Chem.* **1989**, *93*, 6692.

MA702350R